Rev. Roum. Sci. Techn.– Électrotechn. et Énerg.
Vol. **71**, *3*, pp. 391–396, Bucarest, 2026

IOT-BASED ENERGY MANAGEMENT SYSTEM IN ELECTRIC VEHICLES USING OPTIMIZED DEEP LEARNING

SWORNA SHAINI [1], JOSEPH JAWHAR [2]

Keywords: Electric vehicles (EVs); Power demand; Optimization; Deep learning; Battery lifetime.

Electric vehicles are becoming the backbone of smart mobility in smart city applications because of their potential to reduce carbon footprints. In this research, an IoT-based energy management system for EVs by combining the harbor seal whisker optimization (HSWO) and the improved Elman spike neural network (IESNN) has been proposed. The proposed method uses voltage and current sensors on the battery and supercapacitor to transmit real-time energy parameters to the Blynk IoT platform for remote control and monitoring. The proposed IESNN method is used to predict system power demand. Moreover, HSWO is used to tune the network's weight parameters to improve prediction accuracy. IoT integration enables predictive maintenance and real-time data monitoring, enabling users to remotely assess motor performance, energy usage, and battery health. Compared with existing techniques, HSWO-IESNN improves SoC by 11.9%, 9.3%, 7.3%, 5.6%, and 4.4% over IWHO-DL, SCSO-RERNN, EMCABN-ROA, MRA-SDRN, and FBPINN-SAO, respectively.

1. INTRODUCTION

With the development of technology and science, the automobile has evolved from an invention to a mass-produced vehicle that is now a necessary mode of transportation for all families [1]. As the number of EVs increases, more electricity is needed to charge them. The transformer and other distribution system components are put under more strain as EV penetration rises [2, 3]. EV charging stations can be made even more energy efficient by combining renewable energy sources with switchable glass [4, 5].

Nowadays, the Internet of Things (IoT) is an interesting field of study [6]. The Internet of Things is a rapidly evolving and extensively used network in which every electronic gadget in our environment may be connected to every other device to form conversations [7]. Energy flow between solar PV panels and switchable glazing can be adjusted by IoT-based energy management systems in real-time, considering variables like weather, energy demand, and battery condition [8]. This ensures that the EV charging station's energy use is optimized to reduce operating expenses and grid dependence [9]. IoT technologies, including smart sensors, meters, and controllers, are utilized in EV charging stations to gather information on energy production, storage capacity, and usage trends [10].

Numerous methods have been proposed for energy management systems; however, they affect high-power vibration and the battery's high discharge power [11]. The identified research gaps highlight shortcomings of existing energy management techniques, including computational complexity, inaccurate power demand prediction, high cost, and inadequate control of electric vehicles [12]. To overcome these challenges, a novel technique, IoT-based EMS for EVs using deep learning, has been proposed. The following is the main contribution of the proposed method:

- The novelty of this study is the integration of the improved Elman spike neural network (IESNN) and harbor seal whisker optimization (HSWO), HSWO-IESNN, to optimize the EMS in electric vehicles with IoT.
- An IESNN model is specifically designed to capture short-term temporal variations in EV power demand with lower computational complexity than LSTM- and CNN-based models.
- HSWO algorithm is introduced to optimally tune IESNN weight parameters, achieving a superior exploration–exploitation balance compared to PSO, GA, and WOA, thereby significantly improving prediction accuracy.
- The integration of IoT enables real-time data monitoring and predictive maintenance, enabling users to check battery health, energy consumption, and motor performance remotely.

Furthermore, the remainder of the section is as follows: Section 2 explains the related work, and Section 3 discusses the proposed approach. Section 4 provides an analysis of the experiments, and Section 5 presents the article's conclusion and outlines future research.

2. LITERATURE SURVEY

Vasanthkumar, P. *et al*. [13] suggested an enhanced wild horse optimizer with DL based BMS (IWHODL-BMS) in 2022 for IoT-based hybrid EV. Under various measures, a thorough simulation result demonstrated the improved results of the proposed technique over the other approaches. In 2024, Srinivasan, C. [14] suggested an integrated Sand cat swarm optimization and recalling enhanced recurrent neural network (SCSO-RERNN) for HESS control strategy and energy allocation in EVs. The proposed method is put into practice, and its feasibility and effectiveness are confirmed using MATLAB.

In 2024, Kranthikumar, I. et al. [15] suggested a hybrid approach for energy management that integrates the Enhanced Multi-Head Cross Attention-based Bi-LSTM Network with the Remora Optimization Algorithm (ROA). Shanmugam, C. *et al*. [16] presented a Binary Waterwheel Plant Optimization and Prediction that utilizes a Multi-Fidelity Physics-Informed DNN (BWPOA-MFPIDNN) in 2024. Experimental findings depict that the introduced strategy not only offers a more economical option but also greatly extends battery life compared to the prior approach.

Kannayeram, G., et al. [17] presented a hybrid approach in 2024 called the MRA-SDRN technique for maximizing EV charging using renewable energy in an IoT system. Experimental results illustrate the efficacy of the proposed technique, which improves the sustainability, efficiency, and reliability of the IoT. Aruna, P. et al. [18] presented a hybrid method in 2025 that integrates the Snow Ablation Optimizer and the Finite Basis Physics-Informed Neural Network (FBPINN-SAO). The findings unequivocally illustrate that the suggested approach surpasses the current techniques.

In 2025, Djemai, N. et al [19] proposed a physics-based

[1] Department of Electrical and Electronics Engineering, Arunachala College of Engineering for Women, Manavilai, Nagercoil, Tamil Nadu 629203, India. E-mail: swornashaini@arunachalacollege.com (corresponding)
[2] Department of Electronics and Communication Engineering, Arunachala College of Engineering for Women, Vellichanthai, Kanyakumari District, Tamil Nadu, India. E-mail: principal@arunachalacollege.com

DOI: 10.59277/RRST-EE.2026.3.9

and learning systems approach to enhance fuel cell hybrid electric vehicles (FCHEVs) for better performance control and efficient power source operation. The performance of the suggested approach is evaluated through a comparative evaluation of the developed algorithms using various visual and numerical metrics. DUIRASAMY, R. and Thiyagarajan, V., [20] proposed a generalized 13-level symmetrical topology to meet the power quality requirements. It has twelve semiconductor devices and six DC sources. The suggested topology is examined by MATLAB/Simulink, and the hardware prototype has been put into practice in the lab to verify the simulation results. To increase the effectiveness of the onboard battery charger, Malar, J.G. et al. [21] suggested a fractional-order sliding mode controller (FOSMC) for power converters in 2023. The FOSMC parameters are determined by the Harris Hawks optimization (HHO) algorithm. Compared to current techniques like SSA-PID and SSA-FOAFPIDF controllers, the suggested method increases efficiency by 98%.

3. PROPOSED METHODOLOGY

In this section, a novel IoT-based energy management system (EMS) for electric vehicles is presented by combining the Harbor Seal Whisker Optimization and Improved Elman Spike Neural Network (HSWO-IESNN). The performance of a BLDC Motor can be enhanced by generating an optimal PWM duty cycle using the proposed method. The aim is to regulate the inverter switching so that the motor achieves minimum speed error, reduced torque ripple, and improved efficiency. The overall block of HSWO-IESNN is depicted in Fig. 1.

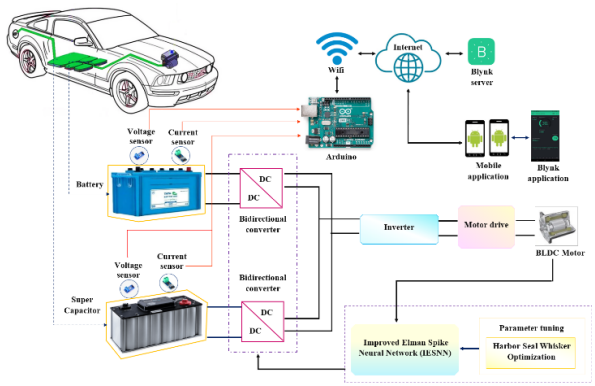

Fig. 1 – Proposed IODL-EMS method.

3.1. CONFIGURATION OF EMS IN EV

Figure 1 shows the EMS setup with IoT, comprising a battery, BLDC motor, and supercapacitor (SC) that serve as the power sources in EVs. Furthermore, the battery and the SC are linked to the bidirectional DC-DC converter.

3.1.1. Battery model

In this study, a Li-ion battery design is used for an EV with a 5Ah capacity and a 300V rated voltage; a power Li-Ion battery is chosen as the backup energy source. Accordingly, it is possible to solve the current i_y inversely and get the output power P_y as follows:

$$P_y(SoC) = B_O(SoC)\times i_y - i_y^2 \times$$
$$\times B_r(SoC) i_y \frac{B_O(SoC) - \sqrt{B_O^2(SoC) - 4\times B_O(SoC)\times P_y(SoC)}}{2\times B_r(SoC)} \quad (1)$$

Here, B_O and B_r the internal resistance of the battery and the open-circuit voltage. The developed EMS must take the battery *SoC* into account when using the Coulomb counting method in this research.

$$SoC(t) = SoC_{to} \int_{\frac{to}{3600h}}^{t} i_y \mathrm{d}t \quad (2)$$

In this case, h represents the battery's rated capacity. $SoC(t)$ is the *SoC* value at time t, and SoC_{to} denotes the battery's starting *SoC* value.

3.1.2. Super capacitor model

Batteries and supercapacitors (SCp) operate on the same concept. The capacitor C in the SC circuit is connected in series with the corresponding resistance. The *SoC*, which influences the supercapacitor's charging and discharging behavior, is a function of time given as;

$$SoC_{\mathrm{SCp}} = SoC_{\mathrm{SCpini}} - \frac{1}{C}\int_0^t I_{\mathrm{SCp}}\, \mathrm{d}t\,. \quad (3)$$

Here, C represents the capacitor's capacity, SoC_{SCpini} represents the supercapacitor's initial state of charge at $t = 0$ s. It exhibits positive and negative current values because of the charging and discharging stages.

3.1.3. Bidirectional DC-DC converter model

Boost-boost half-bridge converters are efficient bi-directional converters because they work as both buck converters when charging and boost converters when discharging supercapacitors (SCp),

$$V_{DD-link} = \frac{1}{1 - U_{boost}} V_{\mathrm{SCp}}, \quad (4)$$

where U_{boost} represents the boost converter's duty cycle, $V_{dc-link}$ represents the voltage at the DC-link, and V_{SCp} represents the voltage across the supercapacitor (SCp).

$$I_{L(avg)} = \frac{I_{load}}{1 - U_{boost}}. \quad (5)$$

I_{load} indicates the current of the converter load, while $I_{L(avg)}$ indicates the average current passing through the inductor. One can calculate the critical inductance of the converter as follows:

$$L_{crit} = \frac{V_{\mathrm{SCp}} U_{boost}}{\Delta I_L s_f}, \quad (6)$$

where L_{crit} is the minimal inductance needed for the converter to operate steadily, ΔI_L is the variation in the inductor current during the switching duration, and s_f is the converter's steady-state switching frequency. The low-voltage side (LVS) capacitance at the input and the high-voltage side (HVS) output capacitance can both be calculated as follows:

$$L_c = \frac{V_{\mathrm{SCp}} U_{boost}}{8 L s_f^2}, \quad (7)$$

$$C_O = \frac{(1 - U_{boost})(U_{boost} I_{L(avg)})}{\Delta V_O s_f}, \quad (8)$$

where $I_{L(avg)}$ denotes the average current that passes through the inductor, ΔV_0 stands for the voltage shift associated with the high-voltage side, L is the converter's inductance, C_O is the HVS output capacitance, and L_c is the LVS input capacitance.

3.1.4. BLDC model

A brushless DC BLDC motor consists of three stator winding stages 120 degrees apart. A DC motor without a brush has electrical dynamics that fulfill a related voltage.

$$\tau_{pqr}^{z} = \frac{\mathrm{d}}{\mathrm{d}t} \times \left(F_{pqr}^{z}\right) + \gamma^{z} \times \varphi_{pqr}^{z}, \quad (9)$$

where τ denotes the stator voltage, γ represents the stator resistance, φ is the stator current. Moreover, parameters are given in a vector form as $F_{pqr}^{s} = [F_{pq} \times F_{qr} \times F_{rs}]$, the flux connection is defined by F, and the stator voltage is present between the neutral points of the motor winding and the current.

3.1.5. Driving cycle

Driving cycles are primarily intended to evaluate emission levels and driving range, as well as to describe the relationship between electric car (EV) speed and time. Nevertheless, they are commonly employed to imitate real-world driving circumstances. Four general categories can be used to group these specifications:

Rolling resistance force (R_{sf}). The friction between the EV tires and the road surface creates the rolling resistance force. This force, which resists vehicle motion, is mostly affected by the mass of the vehicle, the tires, and the state of the road.

$$R_{sf} = R_k mg\cos\theta, \quad (10)$$

where m is the total mass in kg, R_k is the rolling resistance coefficient, θ is the slope angle of the road in degrees, and g is the gravitational constant, which is 9.8 $\mathrm{m/s^2}$.

Aerodynamic resistive force (F_a). The aerodynamic force is generated due to friction between the moving EV and the surrounding air. This resistive force increases significantly with vehicle speed and represents a major source of energy loss at higher velocities. Aerodynamic losses are typically modeled as a function of vehicle speed.

$$A_{rf} = \frac{1}{2}\rho D_c F_a v^2. \quad (11)$$

F_a stands for electric vehicle surface area $\mathrm{m^2}$, D_c for the drag power parameter, ρ represents the density of air in $\mathrm{kg/m^2}$, and v denotes the linear speed of the EV in m/s.

Wheel dynamics. The wheel's rotational motion can be represented as follows, where J_{wheel} and r_{wheel} represent the wheel's moment of inertia and radius, respectively, and ω denotes its rotational speed.

$$J_{wheel}\frac{\mathrm{d}\omega}{\mathrm{d}t} = T_d - r_{wheel}F_d. \quad (12)$$

Here, F_d and T_d indicate the driving force and motor torque, respectively.

3.1.6. Objective function

The objective function of the proposed method is defined as minimizing battery discharging power (MBP), reducing power fluctuations (RPF), maintaining the supercapacitor (SC) in an optimal operating range, and minimizing cost (c). The mathematical equation of the function is defined as;

$$k\big(p(t), w(t), \Delta w(t)\big) \equiv \alpha_1 \times k\big(w(t)\big) + \alpha_2 \times k\big(\Delta w(t)\big) + \alpha_3 \times k\big(p(t)\big), \quad (13)$$

where $\Delta w(t) \equiv [SoC_{battery}(t), SoC_{SCp}(t)]$ is the system state variable and $w(t)$ is the power of the battery; $\alpha_1, \alpha_2, \alpha_3$ represents the cost function's trade-off factors.

$$c = c_{battery} + c_{SCp} + c_{BLDC} + c_{ardunio}, \quad (14)$$

where c shows the total cost of operations, $c_{battery}$ denotes the cost of the battery, c_{BLDC} denotes the cost of the BLDC motor, c_{SCp} denotes the supercapacitor cost, and $c_{ardunio}$ denotes the Arduino controller cost.

3.2. IESNN-HSW BASED ENERGY MANAGEMENT STRATEGY

In this research, the IESNN-HSW technique has been utilized for an energy management system. Conventional optimization-based EMS strategies typically employ algorithms such as genetic algorithms, particle swarm optimization, or rule-based control for parameter tuning. Although these methods can improve energy distribution, they often suffer from slow convergence, local optimum trapping, and limited adaptability to dynamic driving conditions.

To address these limitations, the proposed approach integrates HSWO with an ENN. The theoretical motivation of this framework lies in combining the global search capability of bio-inspired optimization with the temporal dynamic learning ability of recurrent neural networks. The whisker-based sensing mechanism of HSWO enhances exploration and exploitation during the optimization process, enabling efficient tuning of neural network weights. Meanwhile, the ENN captures time-dependent relationships among system variables such as speed error, torque demand, and battery State of Charge.

3.2.1. Prediction *via* improved elman spike neural network (IESNN)

Electric vehicle (EV) battery power demand prediction is modeled and predicted using the IESNN approach. The nodes and input layer are depicted as follows

$$q_x(a) = h_x\big(net_x(a)\big); x = 1, \quad (15)$$

$$net_x(a) = w_x(a), \quad (16)$$

$w_x(a)$ denote the input (battery state of charge (SoC), SCp SoC, historical power consumption data), $q_x(a)$ denotes the initial layer output. IESNN power demand prediction is labeled in eq. (17),

$$S_v(q) = N_F\left(Z_{con*inv}S_{v_{con}}(q), Z_{in*inv}input\ (q)\right), \quad (17)$$

$$S_{v_{conv}}(q) = \delta(q)S_{v_{con}}(q-1) + Z * S_v(q-1), \quad (18)$$

$$input\ (q+1) = Z_{in*out}S_v(q), \quad (19)$$

where N_F is a non-linear function of power demand, $S_v(q)$ and $S_{v_{conv}}(q)$ are represented by the state node vector for the hidden and contextual layers, respectively. $Z_{con*inv}$ denotes the self-connecting feedback gain, Z_{in*out} indicates neurons that have weighted the invisible to output levels, and Z_{in*inv} indicates neurons that have linked the numerical value of each layer. The hidden layer node is expressed by,

$$q_y(b) = K\left(net_y(a)\right); y = 1, \dots 9, \quad (20)$$

$$net_y(b) = \sum_x Z_{in*inv} * q_x(b) + \sum_l Z_{in*inv} * q_l(b); l = 1, \dots 9, \quad (21)$$

where $K\left(net_y(a)\right)$ is the sigmoid function, $q_x(b), q_l(b)$ are the input and hidden layers, and $q_y(b)$ is the hidden layer's result.

$$q_l(b) = \delta q_l(b-1) + q_y(b-1). \quad (22)$$

In this case, δ denotes the feedback gain. At the end of the output layer, the nodes of the layer are shown as

$$q_t(b) = h_t\big(net_t(a)\big), \quad (23)$$

where the parameter influenced by the IESNN method power prediction that is presented is denoted by $q_t(b)$. The delta function of neurons is denoted as α_f , and it is calculated using

$$\alpha_f = \frac{E}{\sum_{x=1}^{Niv}\sum_{q}^{NoD} Z_{inv*out}^{q} \frac{\rho_{input}}{\rho T}}. \quad (24)$$

The following formula (25),

$$E = d_f^{ns} - T_f^{nas}, \quad (25)$$

determines the variation in power demand. Here, d_f^{ns} indicates the predicted duration of power demand spikes T_f^{nas} , and denotes the actual measured power demand variation over time. The IESNN produces the duty cycle $d(t)$ for the inverter PWM,

$$d(t) = f\big(W_i x(t) + W_c h(t-1)\big). \quad (26)$$

The output $d(t)$ controls the PWM of the inverter,

$$V_{out} = d(t) \times V_{dc}. \quad (27)$$

This formulation enables real-time and efficient EV battery power demand prediction using an IESNN.

3.2.2. Optimal tuning *via* HSWO

The IESNN network's performance is enhanced by using the HSWO method to identify the optimal factors for achieving precise detection.

Objective function. To achieve efficient control of the electric vehicle drivetrain, the brushless DC Motor must operate with minimal speed tracking error and reduced torque ripple. Therefore, the HSWO algorithm is utilized to tune the weight parameters of the ENN controller by minimizing a multi-objective cost function.

The speed error objective is expressed using the ISE,

$$J_1(\theta) = \int_0^T w(t)\mathrm{d}t\,. \quad (28)$$

The torque ripple objective function is formulated as

$$J_2(\theta) = \frac{1}{T}\int_0^T (T_e(t) - T_{avg})^2 \mathrm{d}t\,. \quad (29)$$

To simultaneously minimize speed error and torque ripple, a combined optimization objective is defined as

$$J(\theta) = w_1 J_1(\theta) + w_2 J_2(\theta). \quad (30)$$

Exploration stage. Harbor seals use their whiskers at a particular detecting velocity to detect underwater vibrations, which helps them maximize their hunt for prey. It is determined that the seal whisker's detecting velocity is,

$$u_y = \frac{W}{2\pi}\frac{(2p_x^2 - O^2)}{(p_x^2 + O^2)^{5/2}}. \quad (31)$$

$$W = 2\pi\omega l k^3 \sin\omega t\,, \quad (32)$$

where the oscillating sphere diameter is denoted by k, the displacement amplitude by l, and the angular frequency by ω. O denotes the distance between the prey and seal, and p_x represents the seal's location.

Exploitation stage. Depending on their effectiveness they perform in improving forecast accuracy, the Harbor seal's weight parameters are adjusted during the exploitation stage.

$$u_j^{l+1} = Fr_1 u_j^l + aPr_2\big(GP_{best} - Y_j^l\big) + bPr_3\big(FQ_{best,j} - Y_j^l\big), \quad (33)$$

$$F = ba^* \frac{1}{\sqrt{a^2\sin^2 P + b^2\cos^2 P}}, \quad (34)$$

$$b = 0.14\sin(0.92n + 1.5\pi) + 1, \quad (35)$$

$$a = 0.067\sin(0.91m + \pi) - 0.0041m + 0.64, \quad (36)$$

where F represents the ellipse's diameter, r_1, r_2, and r_3 are random numbers, b is the ellipse's major axis length, and a is its minor axis length. The seal is now positioned as

$$Y_j^{l+1} = y_j^l + u_j^{l+1}. \quad (37)$$

The HSWO iteration is considered complete if the ideal weight parameter is chosen after the condition has been updated in the exploitation and exploration phases.

4. RESULT AND DISCUSSION

Experimental results of the proposed HSWO-IESNN strategy and its performance efficacy are covered in this part. The dataset is generated from a MATLAB-based simulation of the EV powertrain and EMS under varying driving conditions. A total of approximately 12,000 time-series samples are collected with a sampling interval of 0.1 s. Each sample consists of input features, including battery SoC, supercapacitor SoC, vehicle speed, traction power demand, and historical power demand values, while the target output is the short-term predicted battery power demand. A 70%–15%–15% ratio is used to divide the dataset into training, validation, and testing. The state-of-the-art method is compared with the MATLAB implementation of the HSWO-IESNN (pro).

Fig. 2 – Experimental test.

Figure 2 illustrates the experimental setup of an electric vehicle prototype, emphasizing its mechanical and electrical control systems. It is a customized motorcycle with a custom-designed DC-DC converter attached to its circuit system. Power management and efficiency enhancement are probably achieved with capacitors, transformers, inductors, and semiconductor switches in this converter.

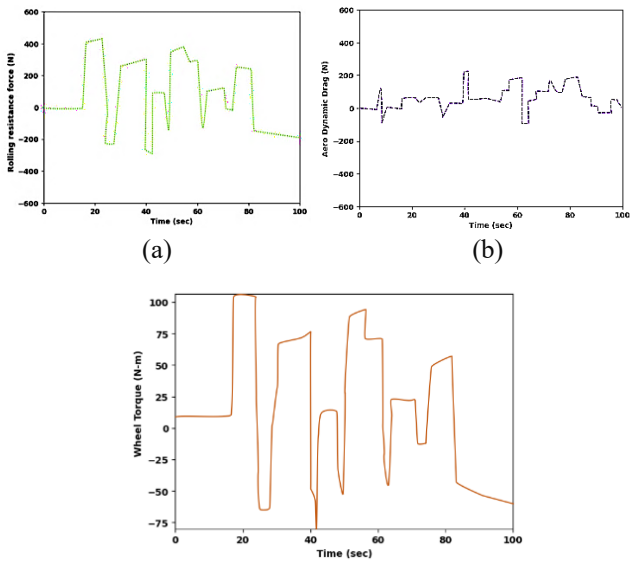

Fig. 3. Analysis: a) rolling resistance; b) aerodynamic; c) wheel torque.

Figure 3 illustrates the external forces acting on the electric vehicle propulsion system that influence the torque demand. In Fig. 3a, the rolling resistance force varies with time due to changes in vehicle speed and road interaction. Higher rolling resistance indicates increased friction between the tire and road surface, which requires additional driving torque.

Figure 3b shows the aerodynamic drag force, which depends on the vehicle speed and air resistance. As speed increases, the aerodynamic drag rises, causing additional load on the motor and increasing energy consumption. Figure 3c presents the wheel torque required to overcome these resistive forces and maintain vehicle motion. The torque fluctuations reflect acceleration, deceleration, and varying load conditions during the drive cycle.

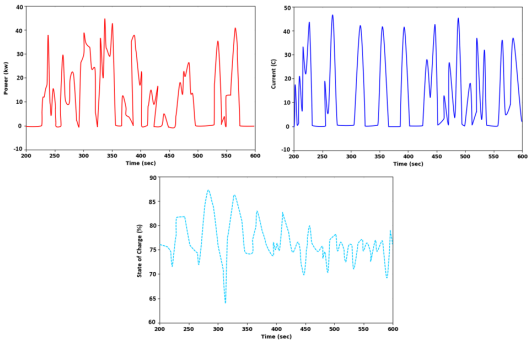

Fig. 4 – Performance of power splitting in the battery (a) speed, (b) Current, (c) State of charge (SoC).

Figure 4 illustrates the dynamic behavior of the battery during power splitting in the electric vehicle system, including (a) speed, (b) current, and (c) SoC of the battery supplying the BLDC Motor. In Fig. 4a, the speed varies according to the driving cycle, indicating acceleration and deceleration conditions of the vehicle. Figure 4b presents the battery current, where sharp current peaks occur during high torque demand periods such as acceleration, while lower current corresponds to steady operating conditions. Figure 4c illustrates the SoC of the battery, which gradually decreases as energy is supplied to the motor. The smooth SoC reduction and controlled current variations indicate that the optimized controller using the proposed method effectively regulates power distribution and improves energy utilization in the electric vehicle system.

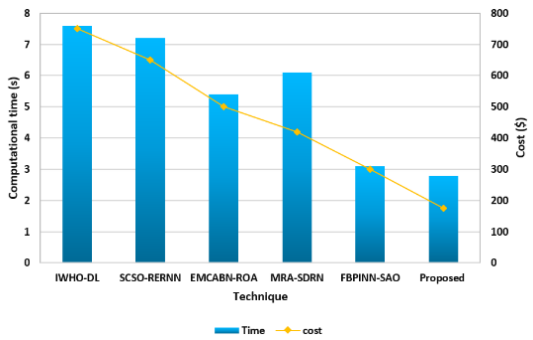

Fig. 5 – Comparison of time and cost in the proposed method with existing methods.

The computation time and operating cost comparison of the proposed and current IWHO-DL, SCSO-RERNN, EMCABN-ROA, MRA-SDRN, FBPINN-SAO, and proposed HSWO-IESNN approaches is shown in Fig. 5. The computational time of HSWO-IESNN (pro) is 2.8 seconds, which is faster than the others. This improvement is primarily attributed to the compact structure of the IESNN, which avoids deep layered architectures, and the fast convergence behavior of HSWO during weight optimization. Physically, reduced computation time implies faster control decisions within the EMS, enabling timely power split adjustments between the battery and supercapacitor.

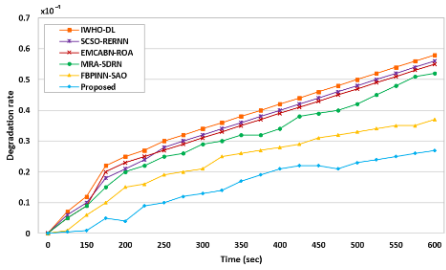

Fig. 6– Capacity degradation comparison of proposed approach

Figure 6 displays the battery systems performance over a long period of time based on the pattern of battery degradation. Battery capacity degradation is strongly influenced by high peak discharge currents, frequent deep cycling, and rapid power fluctuations. The proposed HSWO–IESNN strategy mitigates these stress factors by accurately predicting short-term power demand and dynamically shifting transient power peaks to the supercapacitor. In comparison, existing methods exhibit faster capacity fade due to less precise power prediction and delayed optimization responses, resulting in greater battery stress during prolonged operation.

Table 1

Comparative analysis of response time

Author and year	Methods	Response Time (s)	Efficiency (%)
Vasanthkumar, P. *et al.* (2022)	IWHO-DL [18]	8.9	87.5
Srinivasan, C., (2024)	SCSO-RERNN [19]	8.2	90.6
Shanmugam, C. *et al.* (2024)	EMCABN-ROA [20]	6.3	92.7
Kannayeram, G. *et al.* (2024)	MRA-SDRN [24]	6.8	93.12
Aruna, P. *et al.* (2025)	FBPINN-SAO [25]	3.7	96.77
Ours	Proposed HSWO-IESNN	3.1	98.54

Table 1 presents the response time (in seconds) and efficiency of different methods used in various studies for optimizing computational processes. The IWHO-DL method yields the highest response time of 8.9s, SCSO-RERNN yields 8.2 s, EMCABN-ROA yields 6.3s, MRA-SDRN achieves 6.8 s, while FBPINN-SAO yields 3.7 s, which are all higher than the proposed HSWO-IESNN (3.1 s), respectively. In contrast, methods with longer response times rely on deeper neural architectures or slower-converging optimization algorithms, which delay control actions and increase battery stress. The higher efficiency achieved by the proposed method reflects reduced computational overhead and more accurate power demand prediction, leading to improved utilization of stored energy.

Table 2

Comparison of energy loss and error

Methods	Error (%)	Energy loss (kJ)
Proposed HSWO-IESNN	19.7	2214
FBPINN-SAO	25.4	2345
MRA-SDRN	34.8	2398
EMCABN-ROA	39.14	2465
SCSO-RERNN	41.44	2498
IWHO-DL	42.01	2488

The comparison of the proposed and current methods' energy loss and error is shown in Table 2. At 2214 kJ, the proposed method (HSWO-IESNN) has the least amount of energy loss when compared to the existing models. The

proposed design has a 60% error, which is lower than prior methods. This improvement is mainly due to the smoother power profiles generated by accurate short-term power demand prediction using IESNN and optimal weight tuning via HSWO. Existing methods exhibit higher energy loss due to less accurate prediction and delayed optimization, resulting in frequent high-current battery discharge and increased resistive losses.

5. CONCLUSION

In this research, an IoT-based EMS for electric vehicles is proposed by combining the Harbor Seal Whisker Optimization and Improved Elman Spike Neural Network (HSWO-IESNN). The proposed method uses voltage and current sensors on the battery and supercapacitor to transmit real-time energy parameters to the Blynk IoT platform for remote control and monitoring. The proposed Improved Elman Spike Neural Network (IESNN) model is used for power demand prediction, and the network weight parameters are optimized using Harbor Seal Whisker Optimization (HSWO) to increase prediction accuracy. IoT integration enables predictive maintenance and real-time data monitoring, enabling users to remotely assess motor performance, energy usage, and battery health. MATLAB tool is utilized to estimate the feasibility and effectiveness of the proposed method. The SoC improvement of the HSWO-IESNN method is 11.9%, 9.3%, 7.3%, 5.6%, and 4.4% higher than IWHO-DL, SCSO-RERNN, EMCABN-ROA, MRA-SDRN, and FBPINN-SAO, respectively. Furthermore, the efficacy of the HSWO-IESNN method is 98.54%, which is higher than existing approaches. Future studies should focus on combining blockchain technology with hybrid electric storage systems to increase security.

ACKNOWLEDGEMENTS

The author would like to express his heartfelt gratitude to the supervisor for his guidance and unwavering support during this research for his guidance and support.

CREDIT AUTHORSHIP CONTRIBUTION

SWORNA SHAINI: Study conception and design, analysis and interpretation of results, writing, review and editing

JOSEPH JAWHAR: Data collection, draft manuscript preparation, methodology, writing – original draft

Received on 7 June 2025

REFERENCES

1. T.M. Nair, R.S. Sreelekshmi, M.G. Nair, *Energy management for hybrid energy storage in electric vehicles using neural network*, 2021 Second International Conference on Electronics and Sustainable Communication Systems, pp. 407–411.
2. P. Deepa, S. Rajakumar, P.J. Shermila, E.A. Devi, M.E. Prince, A.J.G. Malar, *New hybrid Cuk-Landsman high gain DC-DC converter modelling and analysis*, Power, **9**, *8*, pp. 8–16 (2022).
3. A.J. Gnana Malar, S. Sellamuthu, M. Ganga, N. Mahendran, S. Hoseinzadeh, A. Ahilan, *Power system planning and cost forecasting using hybrid particle swarm-Harris hawks optimizations*, Journal of Electrical Engineering & Technology, **19**, *2*, pp. 1023–1031 (2024).
4. A.K. Karmaker, M.A. Hossain, H.R. Pota, A. Onen, J. Jung, *Energy management system for hybrid renewable energy-based electric vehicle charging station*, IEEE Access, **11**, pp. 27793–27805 (2023).
5. P. Deepa, S. Rajakumar, P.J. Shermila, E.A. Devi, M.E. Prince, A.J.G. Malar, *New hybrid Cuk-Landsman high gain DC-DC converter modelling and analysis*, Power, **9**, *8*, pp. 8–16 (2022).
6. D. Lavanya, K. Ramakrishnan, *An optimized deep learning based intrusion detection model for network application*, Network Security, **16**, pp. 1–10 (2024).
7. S. Syafii, K. Krismadinata, M. Muladi, T.K. Agung, D.A. Sandri, *Simple photovoltaic electric vehicles charging management system considering sun availability time*, Journal of Sustainable Development of Energy, Water and Environment Systems, **12**, *1*, pp. 1–10 (2024).
8. G. Murugaiyan, J. Gnanamalar, M. Narayanaperumal, V. Muthuvel, *Red fox-based fractional order fuzzy PID controller for smart LED driver circuit*, Rev. Roum. Sci. Techn. – Électrotechn. et Énerg., **68**, *4*, pp. 395–400 (2023).
9. J. Hu, Y. Lin, J. Li, Z. Hou, L. Chu, D. Zhao, Y. Zhang, *Performance analysis of AI-based energy management in electric vehicles: A case study on classic reinforcement learning*, Energy Conversion and Management, **300**, pp. 1–10 (2024).
10. M. Devaki, J. Sathiamoorthy, M. Usha, *IoT based air quality monitoring using DenseNet in urban areas*, International Journal of Data Science and Artificial Intelligence, **2**, *4*, pp. 121–127 (2024).
11. X. Sun, J. Fu, H. Yang, M. Xie, J. Liu, *An energy management strategy for plug-in hybrid electric vehicles based on deep learning and improved model predictive control*, Energy, **269**, pp. 1–10 (2023).
12. M.T. Vellingiri, I.M. Mehedi, T. Palaniswamy, *A novel deep learning-based state-of-charge estimation for renewable energy management system in hybrid electric vehicles*, Mathematics, **10**, *2*, pp. 1–10 (2022).
13. P. Vasanthkumar, A.R. Revathi, G.R. Devi, R.J. Kavitha, A. Muniappan, C. Karthikeyan, *Improved wild horse optimizer with deep learning enabled battery management system for internet of things based hybrid electric vehicles*, Sustainable Energy Technologies and Assessments, **52**, pp. 1–10 (2022).
14. C. Srinivasan, *Energy management of hybrid energy storage system in electric vehicle based on hybrid SCSO-RERNN approach*, Journal of Energy Storage, **78**, pp. 1–10 (2024).
15. I. Kranthikumar, C.H. Srinivas, T.V. Kiran, P. Pradeep, V. Balamurugan, *A novel hybrid approach for efficient energy management in battery and supercapacitor-based hybrid energy storage systems for electric vehicles*, Electrical Engineering, **107**, *1*, pp. 1–7 (2025).
16. C. Shanmugam, S. Nattuthurai, S. Muthusamy, *Optimized control of hybrid energy storage systems for electric vehicles using BWPOA-MFPIDNN approach*, Journal of Energy Storage, **104**, pp. 1–10 (2024).
17. G. Kannayeram, R. Muniraj, J.J. Jasmine, S.E. Raja, T. Jarin, *Energy management of renewable energy connected electric vehicles charging using internet of things: Hybrid MRA-SDRN approach*, Energy, **304**, pp. 1–10 (2024).
18. P. Aruna, V.V. Prabhu, V. Krishnakumar, *Innovative optimization of hybrid energy storage systems for electric vehicles: Integrating FBPINN-SAO to enhance performance and efficiency*, Journal of Energy Storage, **108**, pp. 1–10 (2025).
19. N. Djemai, A. Arif, A. Guettaf, T. Berghout, *Physics-informed representation learning for hybrid electric vehicle energy management*, Rev. Roum. Sci. Techn. – Électrotechn. et Énerg., **70**, *4*, pp. 579–584 (2025).
20. R. Duirasamy, V. Thiyagarajan, *A novel fault-tolerant generalized symmetrical topology for renewable energy and electric vehicle applications*, Rev. Roum. Sci. Techn. – Électrotechn. et Énerg., **69**, *4*, pp. 383–388 (2024).
21. J.G. Malar, V. Thiyagarajan, N.B.M. Selvan, M.D. Raj, *Electric vehicle onboard charging via Harris hawks optimization-based fractional-order sliding mode controller*, Rev. Roum. Sci. Techn. – Électrotechn. et Énerg., **68**, *1*, pp. 30–35 (2023).